Simulation of Wind Generation Data for the WAPA Wind Integration Study

Michael C. Brower
Principal, AWS Truewind, LLC
April 25, 2005

Introduction

Under subcontract to ABB, Inc., AWS Truewind has provided wind data to enable ABB to study the potential impacts on the WAPA grid of wind energy projects in seven areas of North and South Dakota. The wind data consist of simulated one-hour average plant production values for 2003 and for a typical historical year at 65 prospective wind project sites totaling 3816 MW of wind plant capacity. The sites were chosen by a site-screening program developed by AWS Truewind, using as inputs wind resource estimates produced by AWS Truewind's MesoMap system, a 1.5 MW turbine power curve, transmission line locations, and other pertinent data. This report describes the method used to map the wind resource, select the sites, and produce the wind generation data, and describes the results of the validation of the simulated data.

Wind Resource Mapping

The first major task was to map the wind resource in the seven areas shown in Figure 1. We used the MesoMap system, which was developed by AWS Truewind for the mapping of wind resources over large regions with high resolution. MesoMap characterizes wind resources in a region by recreating actual weather and wind conditions for 366 days randomly sampled from a 15-year historical record. The key inputs are reanalysis and rawinsonde data, which provide a snapshot of atmospheric conditions at regular time intervals throughout the world over the past several decades. For each day in the sample, the wind speed and direction (as well as temperature, pressure, precipitation, cloud cover, and other meteorological variables) are simulated and stored at hourly intervals over the model domain at multiple levels above the surface. When the runs are finished, the data are compiled and summarized to produce maps of mean wind speed and wind power density as well as data bases containing wind speed and direction distributions.

After the maps were produced, the mean speeds were validated by comparison with data from 49 airports and tall towers in both states. The observed speeds were first projected to a height of 50 m to provide a consistent basis for comparison. We found that the map underestimates the mean wind speed by an average of about 2%, with a standard error of 4%. This rate of error is typical for MesoMap projects, and we determined that no map adjustments were needed.

Site Selection

The next task was to select likely sites for future wind projects. The site selection was done using methods and software developed by AWS Truewind for site prospecting.

First, wind speed frequency distributions and temperature data generated by the MesoMap system were used to predict the average annual gross energy output of a 1.5 MW wind turbine at every point on the map. The GE 1.5s turbine with 65 m hub height was assumed for this purpose. The gross output was then reduced by 14% to account for typical rates of turbine availability and

electrical, wake, icing, and other losses for projects in this climate. The result was a map of the predicted average net capacity factor in each area.

Exclusion areas, including federal and state parks, locations within 1 mile of a designated dwelling or populated area, water bodies, and slopes greater than 20%, were then identified and mapped. A vector layer of the existing transmission and distribution grid (voltages of 115 kV and up) was overlaid on the other layers, and the minimum cost to connect any point on the map to the existing grid, while avoiding excluded areas (except steep slopes), was calculated.

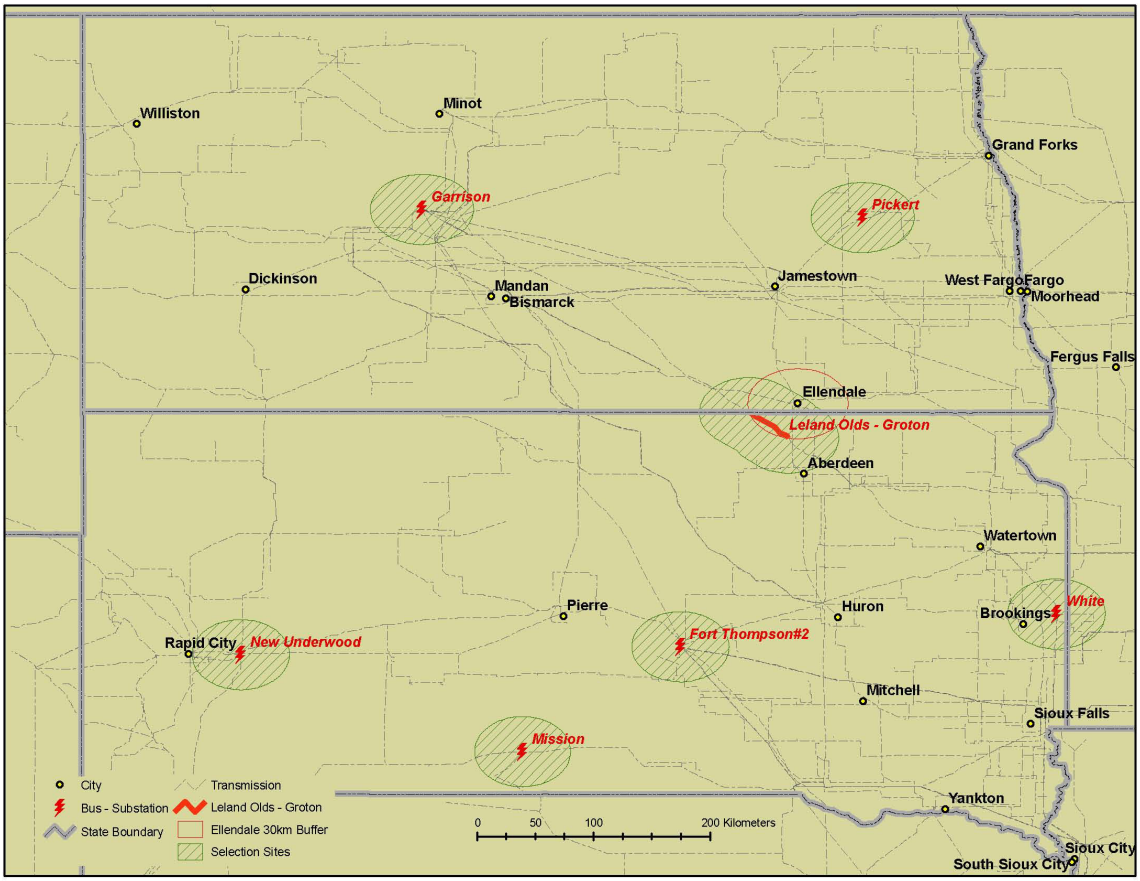

Figure 1. The seven areas in which potential wind project sites were selected.

Using the various GIS data layers created up to this point, we ran a program to select sites that would provide the lowest cost of energy (COE) within a sufficiently large area to support a wind project of at least 50 MW rated capacity. The COE (in $/kWh) was calculated using the following equation:

$$COE = \frac{FCR \times (CC \times MW + TC + SC)}{8760 \times CF \times MW} + OM$$

where

FCR = fixed charge rate (or levelized cost of capital)
CC = plant capital cost
MW = plant rated capacity in MW
TC = new transmission cost

SC = new substation cost
CF = net plant capacity factor
OM = levelized operations and maintenance cost

The assumptions initially used by the program to select the sites are shown in the second column of Table 1. The assumptions were later revised based on feedback from the project review committee. The initial O&M cost assumed no production tax credit (PTC); the revised O&M cost includes the PTC. The capital cost has also been reduced. Although the new assumptions have lowered the estimated COE for each site, they have not substantially affected the relative ranking of the sites within each area.

Table 1. Cost assumptions for site screening

Parameter	Initial Assumptions	Revised Assumptions
Fixed Charge Rate	15%	15%
Capital Cost	$1200/kW	$1050/kW
Transmission Cost	$140,000/km	$140,000/km
Substation Cost	$1.9M	$1.9M
O&M	$0.012/kWh	$0.000/kWh

The site-screening program was tuned to produce about 10 sites of at least 50 MW size in each area, with a 5 km minimum spacing between them to ensure some geographic diversity. The characteristics of the sites are summarized in Table 2. The predicted net capacity factors range from 32% to 42%, and the average wind speed from 7.6 m/s to 8.9 m/s. The predicted cost of energy ranges from $0.045/kWh to $0.059/kWh.

Table 2. Site Characteristics

Area	ID	Average Elevation (m)	Average Speed (m/s)	Average Power (W/m^2)	Net Capacity Factor	MW Capacity	COE ($/kWh)
Leland	1	665	8.4	550	0.38	50	0.049
Leland	2	672	8.3	510	0.37	50	0.050
Leland	3	680	8.2	500	0.37	50	0.051
Leland	4	679	8.1	490	0.36	51	0.051
Leland	5	671	8.1	483	0.36	50	0.052
Leland	6	620	8.2	536	0.37	57	0.052
Leland	7	625	8.0	484	0.36	50	0.053
Leland	8	664	8.3	519	0.37	50	0.053
Leland	9	655	8.0	475	0.35	80	0.052
Leland	10	590	8.1	509	0.36	78	0.052
Mission	1	783	8.7	575	0.41	50	0.046
Mission	2	954	8.8	608	0.41	50	0.046
Mission	3	811	8.5	535	0.40	50	0.047
Mission	4	826	8.5	540	0.39	50	0.047
Mission	5	715	8.4	544	0.39	52	0.048
Mission	6	754	8.5	567	0.40	53	0.048
Mission	7	687	8.4	538	0.39	65	0.048
Mission	8	845	8.4	519	0.38	54	0.049
Mission	9	903	8.4	531	0.38	56	0.049
Mission	10	893	8.3	492	0.37	51	0.050
Pickert	1	460	8.0	501	0.37	50	0.051

Area	ID	Average Elevation (m)	Average Speed (m/s)	Average Power (W/m^2)	Net Capacity Factor	MW Capacity	COE ($/kWh)
Pickert	2	462	8.0	504	0.37	58	0.051
Pickert	3	472	8.0	488	0.36	51	0.052
Pickert	4	457	8.0	493	0.36	62	0.052
Pickert	5	455	8.0	496	0.36	65	0.052
Pickert	6	462	8.0	504	0.36	50	0.053
Pickert	7	456	7.8	456	0.35	54	0.053
Pickert	8	458	7.8	457	0.35	87	0.053
Pickert	9	457	7.8	454	0.35	67	0.054
Underwood	1	942	8.2	524	0.36	51	0.052
Underwood	2	908	8.1	492	0.36	54	0.053
Underwood	3	907	8.1	503	0.36	52	0.054
Underwood	4	892	8.0	503	0.35	65	0.054
Underwood	5	863	7.8	478	0.33	51	0.057
Underwood	6	950	7.8	497	0.33	50	0.058
Underwood	7	922	7.8	465	0.32	50	0.058
Underwood	8	979	7.7	480	0.32	50	0.058
Underwood	9	908	7.7	507	0.32	50	0.059
Underwood	10	882	7.6	467	0.32	51	0.059
White	1	605	8.8	694	0.42	50	0.045
White	2	597	8.9	766	0.42	50	0.045
White	3	606	8.7	595	0.41	50	0.046
White	4	609	8.7	616	0.41	58	0.046
White	5	596	8.5	577	0.40	51	0.047
White	6	607	8.5	560	0.40	50	0.047
White	7	595	8.5	552	0.39	50	0.048
White	8	568	8.5	582	0.39	95	0.047
White	9	535	8.6	669	0.40	68	0.047
Garrison	1	642	8.5	575	0.40	50	0.047
Garrison	2	665	8.4	540	0.39	50	0.048
Garrison	3	642	8.5	569	0.40	54	0.048
Garrison	4	699	8.4	533	0.39	51	0.049
Garrison	5	650	8.3	522	0.38	93	0.048
Garrison	6	660	8.2	504	0.38	55	0.050
Garrison	7	638	8.2	500	0.37	80	0.050
Garrison	8	667	8.2	493	0.37	50	0.051
Garrison	9	573	8.1	518	0.36	135	0.050
FtThompson	1	629	8.7	613	0.41	50	0.048
FtThompson	2	654	8.4	518	0.39	66	0.048
FtThompson	3	654	8.3	511	0.38	54	0.049
FtThompson	4	614	8.2	502	0.38	88	0.049
FtThompson	5	622	8.4	522	0.39	101	0.048
FtThompson	6	564	8.2	544	0.38	52	0.050
FtThompson	7	585	8.3	534	0.38	50	0.050
FtThompson	8	609	8.3	495	0.38	50	0.050

In Figure 2, the average capacity factor of the sites in each area is plotted. The most productive sites are predicted to be found in the Mission and White areas; and the least productive in Underwood.

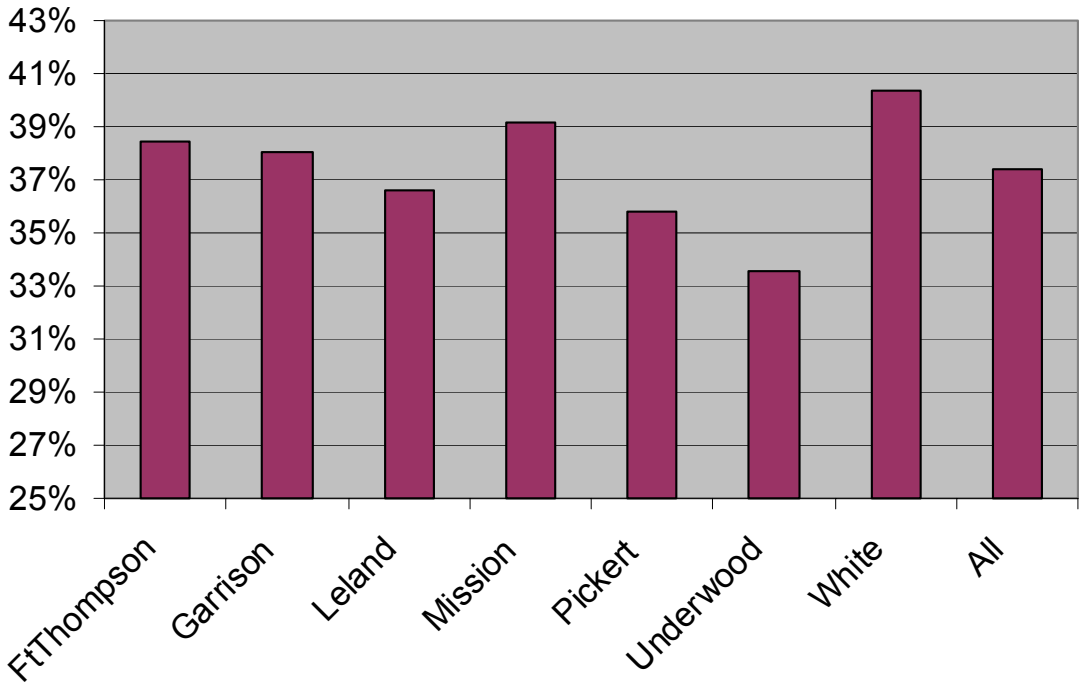

Figure 2. Average net capacity factor of sites in each study area.

Figure 3 depicts a cost-supply curve encompassing all sites in the seven areas. The cost-supply curve is calculated by sorting the sites in order of increasing COE and then plotting the COE against the cumulative megawatts of rated capacity. The mean wind speed does not follow a smoothly decreasing curve because it is not the only factor affecting the COE.

Hourly Average Wind Generation Data

The third task was to simulate two sets of hourly wind generation data for the selected sites. The first set was for a typical historical year, the second for the year 2003.

First, hourly average wind speed and temperature data were extracted from the MesoMap runs for a point at the center of each of the 65 sites. The MesoMap system models the wind climate by simulating 366 complete days of weather from a 15-year period and storing the data at hourly intervals. The days are chosen using a stratified random sampling method so that each month and season is properly represented, but the year is randomized. Thus, the data do not represent a single continuous year, but rather different days from different years.

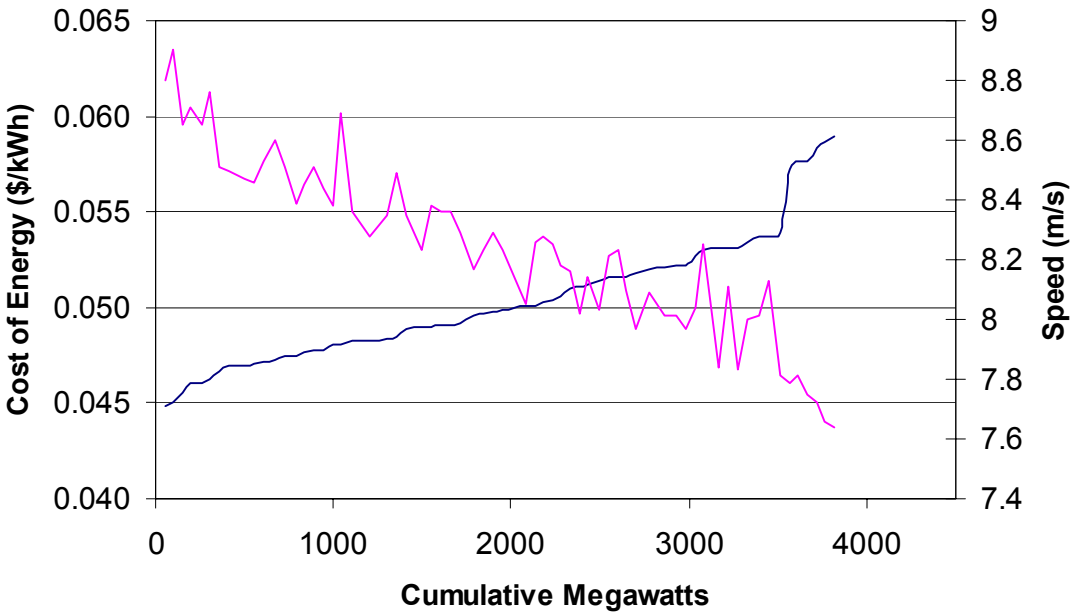

Figure 3. Cost of energy (blue line) and average speed (pink line) versus cumulative megawatts of capacity. The sites have been sorted in order of increasing cost of energy. Although the wind speed is generally higher at sites with a lower COE, other factors, including new transmission costs, the speed frequency distribution, and the air density, affect the COE.

Next the temperature data were converted to hourly air density values. The speeds were then reduced by 6% to mimic turbine wakes, blade soiling, icing, and other losses affecting turbine performance. The adjusted speeds were passed through the GE 1.5s power curve, interpolated to the air density, and 4% was subtracted to account for electrical losses and turbine availability. The effective total loss was about 14%. Last, the output was scaled to the rated capacity for the site. The result was an estimate of the net hourly plant output at each site for a typical historical year.

The MesoMap system was also run for 365 continuous days from 2003, and the same process was applied to produce simulated wind output data for that year.

Figure 4 presents a 31-day sample of the 2003 data generated for two sites in the Leland area and one in the Mission area. The pattern of wide fluctuations in wind output is typical for wind projects. It may be noted that the simulated outputs of the two Leland sites are more highly correlated with one another than they are with the output of the Mission site. This reflects the fact that as the distance scale grows, weather patterns become less coherent in space and time. The dependence of the correlation between sites on distance is depicted graphically in Figure 5.[1] Here the distance is measured with respect to Site 1 in the Leland area, and the correlation is calculated between the hourly output for this site and for each of the other sites. The reduction in correlation with distance depends strongly on the time period over which the data are averaged. The longer

[1] We could find no relationship between the correlation coefficient and distance in a particular direction. We do not believe such a relationship should exist, considering that the correlation measures the frequency of disturbances occurring at different places at the same moment in time. A time-shifted correlation analysis could reveal the passage of weather systems through the region along consistent paths but is beyond the scope of this study.

the averaging period, the higher the correlation at more distant sites, reflecting the fact that large weather disturbances last much longer than small ones.

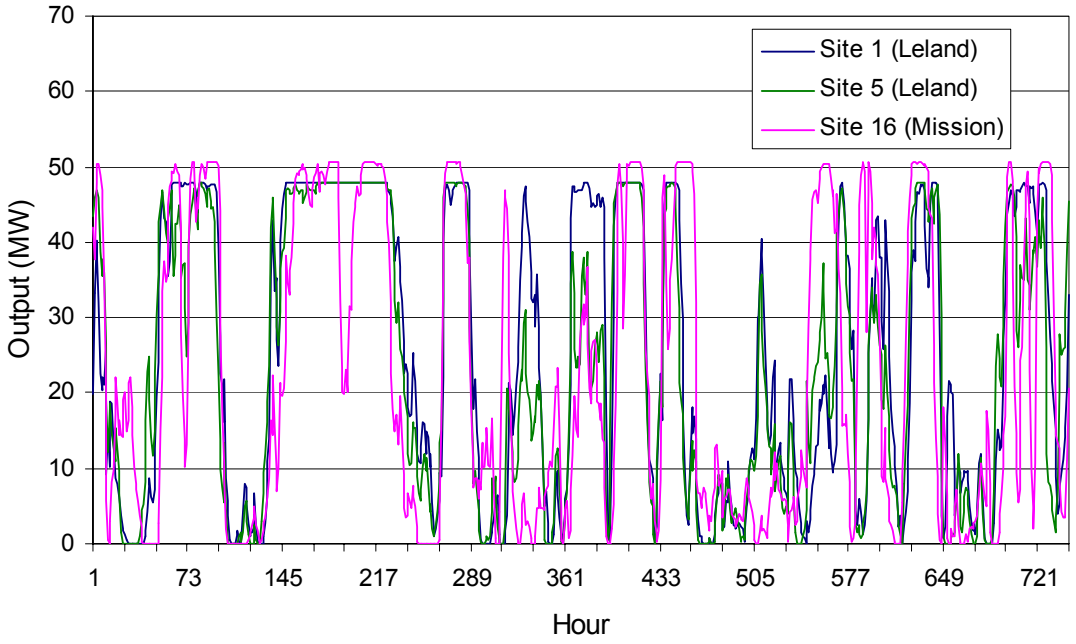

Figure 4. Sample of output from 2003 simulations at three sites.

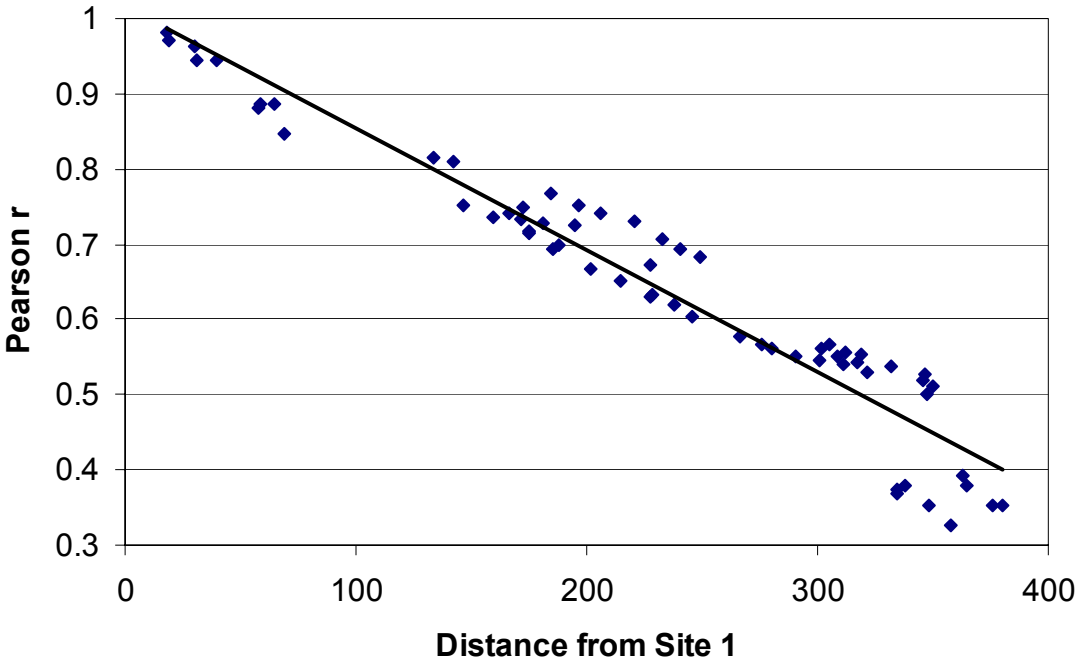

Figure 5. The correlation of simulated hourly output between site 1 and all other sites as a function of distance from site 1.

Wind Speed Validation: Diurnal, Seasonal, and Dynamic Behavior

The last stage of the analysis was the validation of the simulated wind speeds and plant output. The main purpose of this validation was to determine if the simulated data provided a realistic picture of the diurnal, seasonal, and dynamic characteristics of the wind. We did this using wind speed data in AWS Truewind's archives from two tall towers in North Dakota, Olga and Wilton; and wind plant output data provided by Basin Electric Power Cooperative for eight wind projects.[2] The Olga data covered 1995 to 1998, the Wilton data covered 1995 to 1997, and the plant output data covered the month of December, 2004.

First we compared the average diurnal wind speed patterns at Wilton and Olga with the simulated data. Diurnal patterns are useful for estimating average loads during peak periods, an important component of the capacity value. The annual pattern for Olga is shown in Figure 6; the seasonal patterns are shown in Figure 7. The annual and seasonal diurnal patterns for Wilton are depicted in Figures 8 and 9, respectively. Both the observed and simulated patterns indicate rather moderate variation between night and day, with the highest speeds usually occurring from late evening to early morning. At Olga, the simulated speed tends to be too high around 5 am, especially in summer; at Wilton, however, the simulated speed in the early morning tends to be somewhat lower than the observed. Some of these differences may be due to normal statistical fluctuations (as indicated by the error bars), as the simulations and observations cover different time periods. The remaining differences may be due to local influences not resolved by the model as well as possibly to errors in the simulation of the stable nocturnal boundary layer.

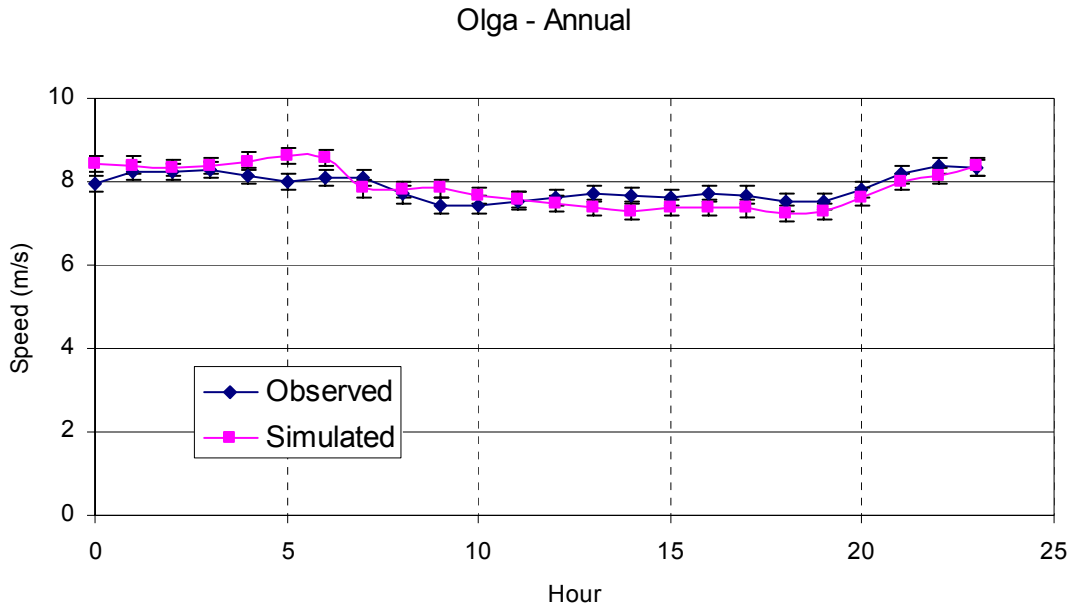

Figure 5. Comparison of simulated and observed annual diurnal wind speed patterns at the Olga met mast at 50 m. The simulated data are for 2003, the observed are for 1995-1998. The error bars reflect the uncertainty in the mean speed due to normal fluctuations.

[2] The eight projects are Chamberlain, Minot, Hyde, Pipestone, Rosebud, Valley City, Edgeley, and Petersburg. The data were provided by Matthew Stoltz, Manager of Transmission Services for Basin Electric Power Cooperative.

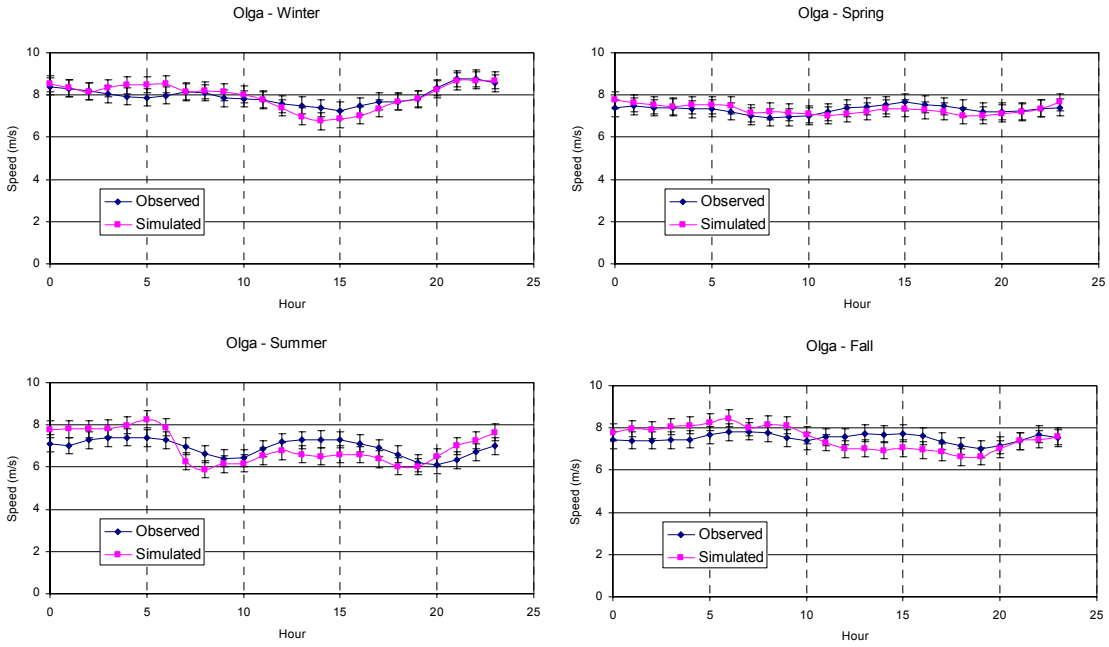

Figure 6. The same as Figure 5 on a seasonal basis.

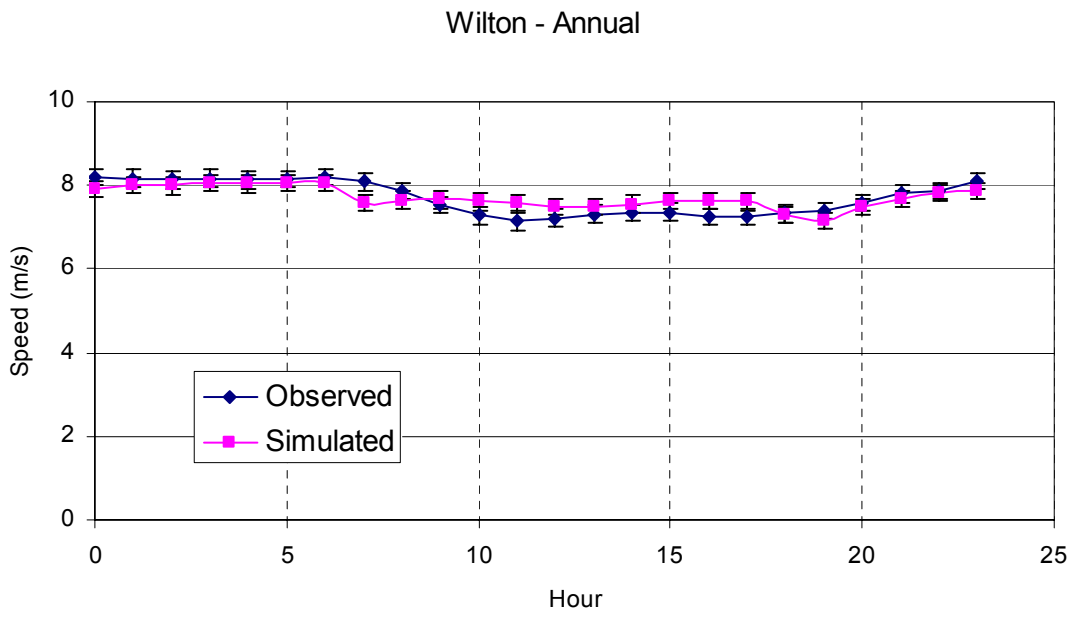

Figure 7. Comparison of simulated and observed annual diurnal wind speed patterns at the Wilton met mast at 50 m. The simulated data are for 2003, the observed are for 1995-1997. The error bars reflect the uncertainty in the mean speed due to normal fluctuations.

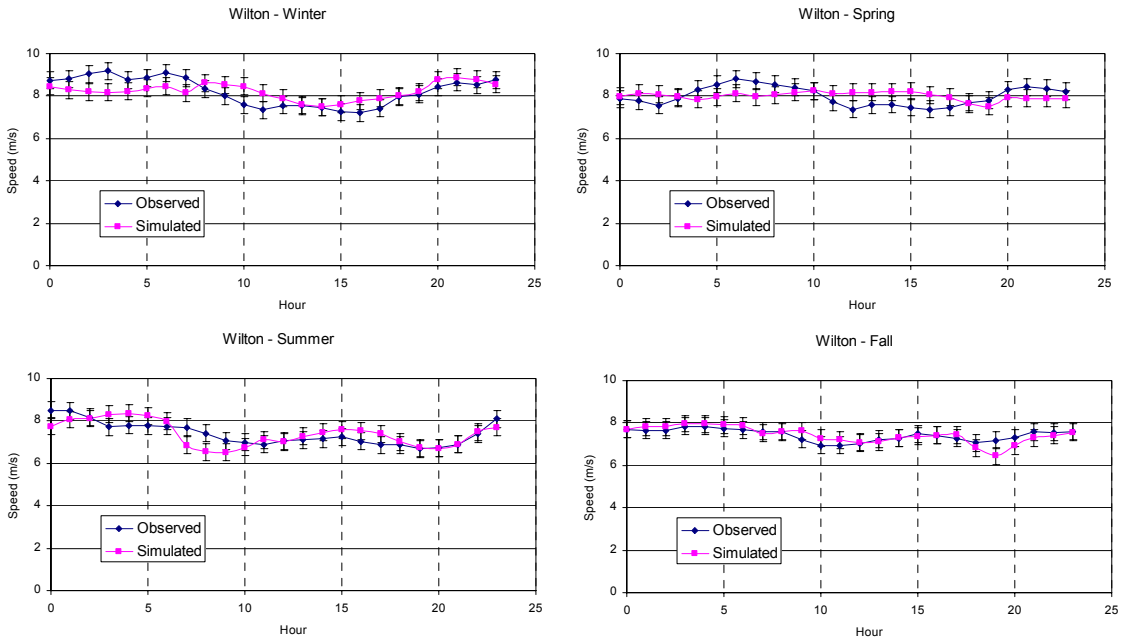

Figure 8. The same as Figure 7 on a seasonal basis.

Next we turn to seasonal variations in mean speed. In Figures 9 and 10, we compare the mean monthly wind speeds at Olga and Wilton with the simulated values. The error bars indicate the normal range of variation. The charts reveal very similar, and for the most part statistically indistinguishable, patterns, with the highest speeds observed from late fall through winter and the lowest from late spring through summer.

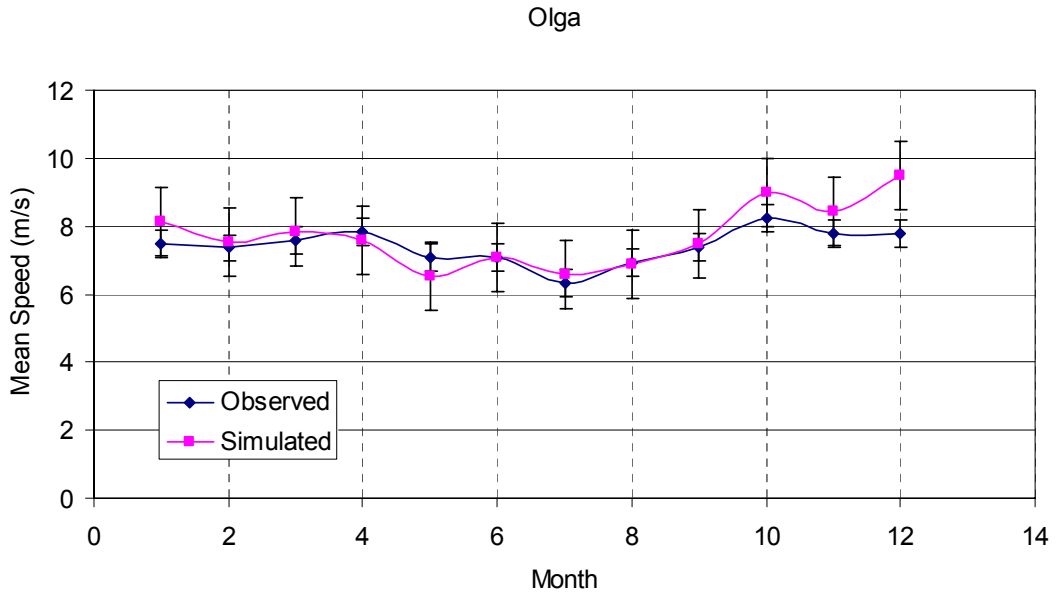

Figure 9. Observed and simulated monthly mean wind speeds at the Olga met mast at 50 m. The simulated data are for a typical year, the observed are for 1995-1998. The error bars indicate the uncertainty associated with year-to-year fluctuations in speed.

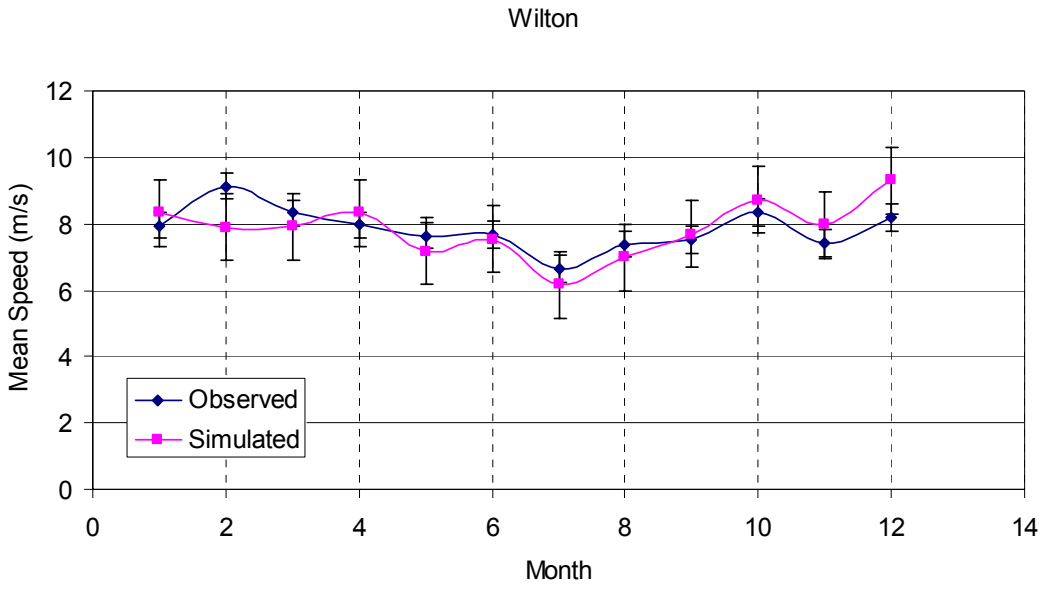

Figure 10. The same as Figure 9 for the Wilton met mast. The observed data are for 1995-1997.

So far we have looked at the mean behavior of the simulated and observed wind speeds. The next stage is to compare their dynamic behavior, or variability, which is important in determining the impacts of wind generation on load-following and other reserve requirements.

First, we compare the speed frequency distributions, shown in Figures 11 and 12. Despite some differences, the distributions on the whole are very similar. The standard error of the bin frequency between 1 and 15 m/s at each mast is 0.5-0.7%. We regard this error rate as minor considering that the simulations and observations cover different time periods.

Second, we compare average changes in wind speed over different time periods. In Figures 13 and 14, the mean absolute deviation in speed is plotted over a range of time steps from 1 to 24 hours for each mast. The agreement between the model and observations at Olga mast is quite close; the variability of the observations is only slightly greater than that of the simulations. At Wilton, the discrepancy is somewhat larger, with the observed variability exceeding the simulated by an average of about 8%. These differences do not necessarily indicate a problem with the simulations. The model and observations represent somewhat different things. The observations are made at a point, whereas the model simulates wind conditions over a 10 km grid cell. Furthermore, there is a tendency for the short-term variability of a wind project's output to be reduced somewhat by the effects of uncorrelated wind fluctuations experienced by the turbines (although the reduction is modest on a 1-hour time scale). The ability of the model to predict the dynamic behavior of wind projects is examined more directly in the next section.

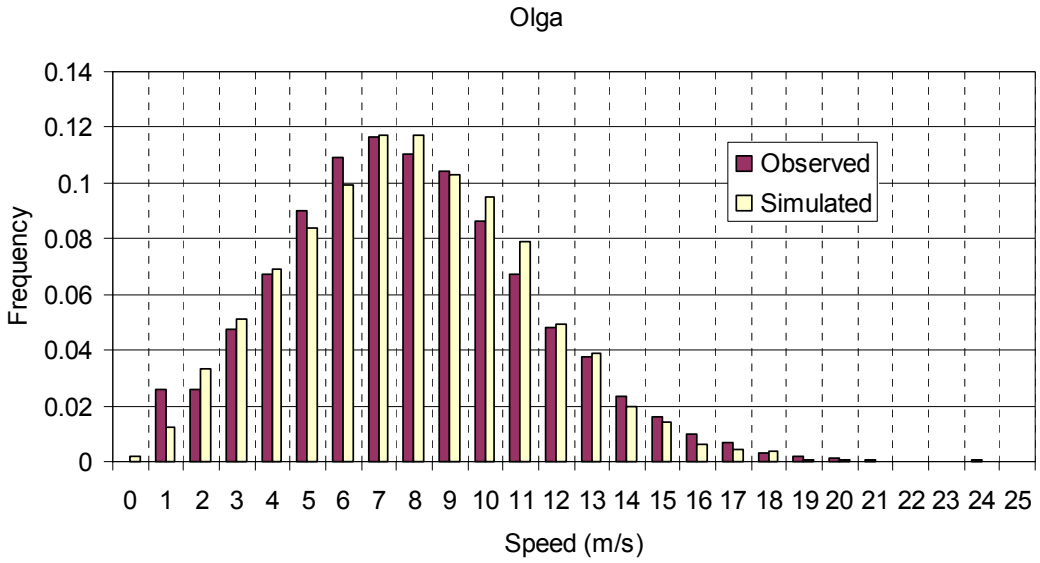

Figure 11. Simulated and observed speed frequency distributions for the Olga met mast. The observed data are for 1995-1998, simulated data are for 2003.

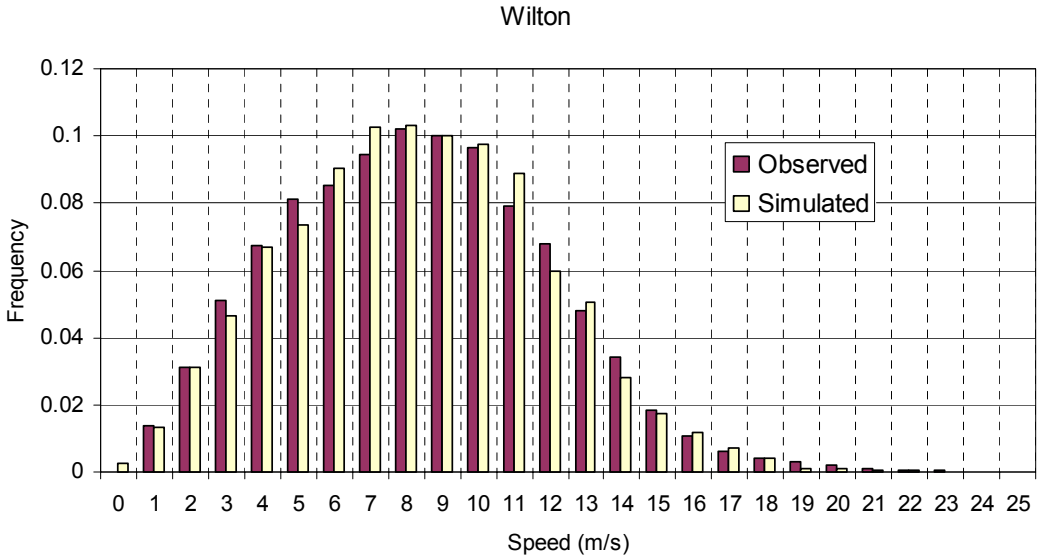

Figure 12. Simulated and observed speed frequency distributions for the Wilton met mast. The observed data are for 1995-1997, simulated data are for 2003.

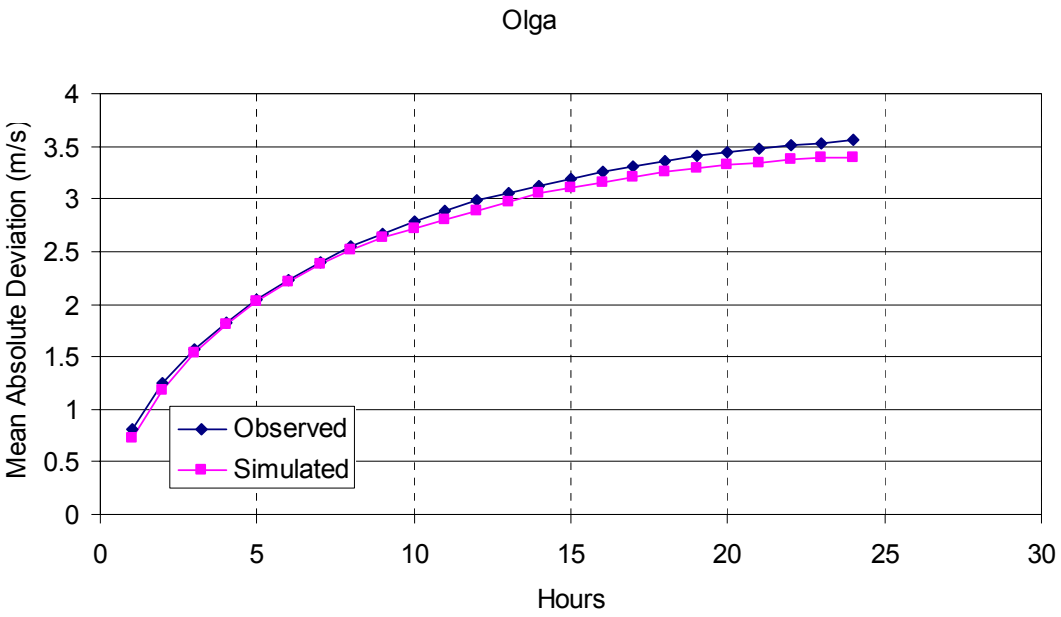

Figure 13. Simulated and observed mean absolute deviations for the Olga mast. The mean absolute deviation is the change in wind speed from time T to time T+N, averaged over all times. The interval N is varied in this plot from 1 to 24. The observed data are for 1995-1998, simulated data are for 2003.

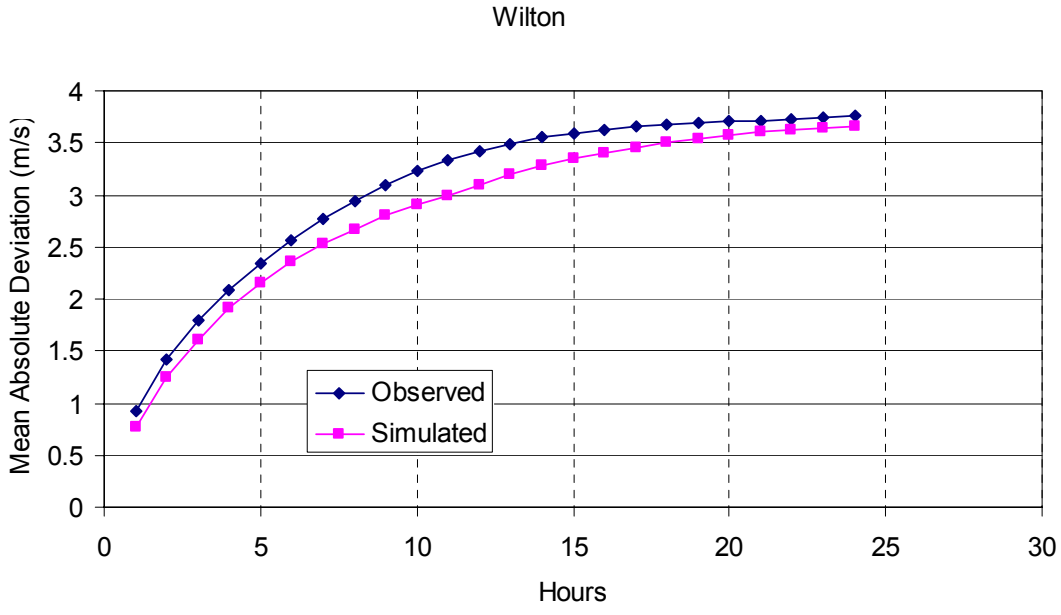

Figure 14. The same as Figure 13 for the Wilton mast.

Wind Plant Output Validation: Diurnal and Dynamic Behavior

To validate the simulated wind plant output we were provided with data for eight wind projects from December 2004. Six of the projects consist of only one or two turbines with 700 kW to 2600 kW total rated capacity, whereas two – Edgeley and Hyde – are sizable wind projects of 40 MW rated capacity each. The data covered December 2004. Since we had only one month, we did not consider the seasonal pattern but only the diurnal pattern and dynamic behavior. In addition, to limit the scope of the effort, we compared the observed data to the simulated data at all 65 sites, without trying to match sites to projects.

Figure 15 plots the observed and simulated diurnal patterns of plant output. The projects and sites have all been scaled to a rated capacity of 50 MW. The average simulated output is obviously higher than the observed. (Possible reasons include project location, turbine type, hub height, and normal year-to-year variations in the monthly mean wind resource.) To provide a more direct comparison of the diurnal patterns, we have scaled the simulated data to match the average observed output for the month. Based on the scaled data, the model appears to do a reasonably good job predicting the average daily pattern, although there may be a tendency to overestimate the average output by about 10% near midday and underestimate it by about 6% in the early morning. The standard error of the hourly means is about 2% of the rated capacity, or 6% of the average output in this period. We regard these differences as falling within the expected uncertainties of the data and method.

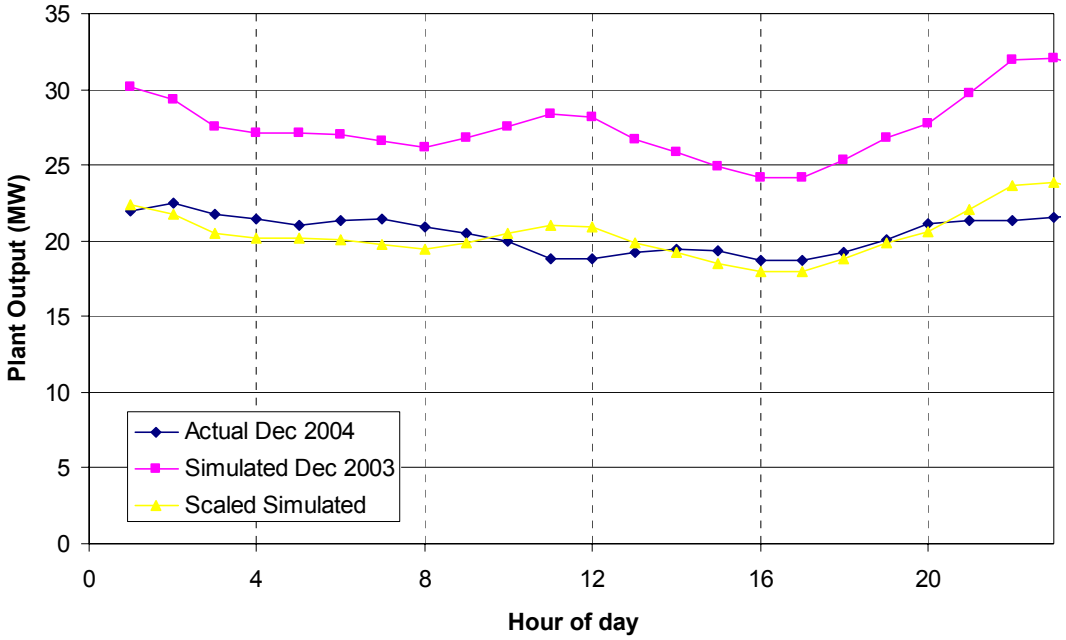

Figure 15. A comparison of the simulated and observed mean wind plant output versus time of day in December. The simulated data are for all 65 sites in December 2003; the observed data are for 8 wind projects in December 2004. To facilitate comparison of the daily pattern, the simulated data have been scaled in the third curve to match the observed output.

In Figure 16, we have plotted the mean absolute deviation of the simulated wind plant output averaged over 65 sites and the observed output averaged over the two 40 MW projects, Hyde and Edgeley. The reason to consider only those two projects is to capture the normal spatial smoothing of the output that occurs in projects of a significant size. The plot shows that the model matches the observed dynamic behavior very closely over time steps of up to 10 hours. Beyond

10 hours, the simulated variability increases somewhat more than the observed, although the discrepancy is consistent with the uncertainty in the observed deviations (which is derived from differences in the mean absolute deviations of the two projects). The results indicate that the model provides a realistic, and perhaps conservatively high, estimate of the dynamic behavior of wind projects in the region.

It may be noted that, whereas the variability of the simulated wind speeds is somewhat lower than that of the observed at the Wilton and Olga met masts (refer to Figures 13 and 14), the opposite appears to be true of the simulated and observed plant data. This difference may reflect the spatial smoothing of the wind fluctuations described earlier, as well as variations in the dynamic characteristics of the wind at different locations.

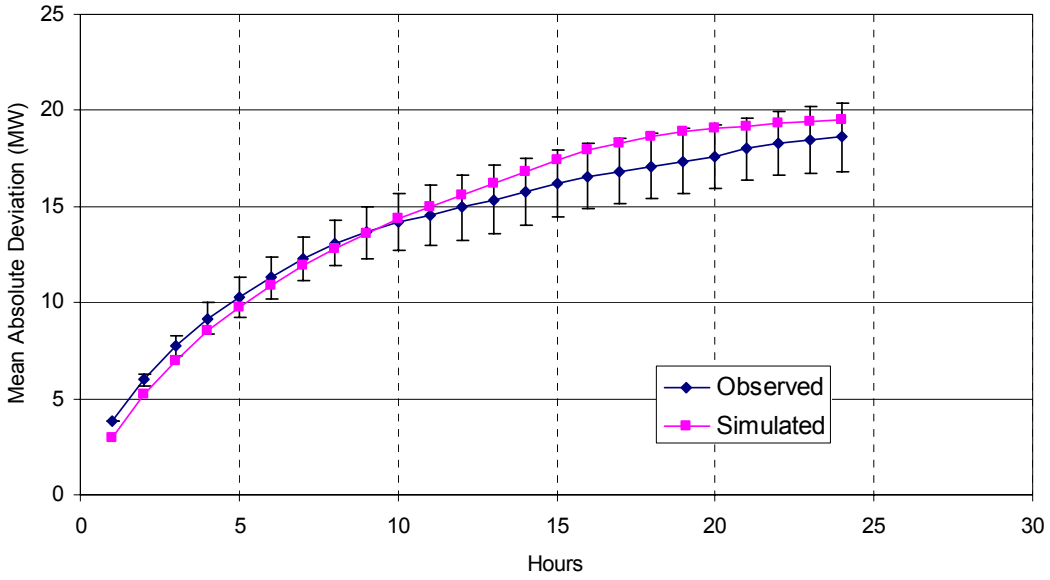

Figure 16. Mean absolute deviation as a function of time of the simulated and observed plant output. The simulated data, which are averaged over all 65 sites, are from December 2003; the observed data are for the Hyde and Edgeley projects from December 2004. Both the observed and simulated data have been scaled to a rated capacity of 50 MW.

Conclusions

AWS Truewind has provided simulated one-hour average wind plant output data for 65 prospective wind project sites in North and South Dakota totaling about 3800 MW of potential wind capacity. The sites are located in seven areas of the two states, with each area containing at least 500 MW. The sites were chosen using wind resource maps of the areas produced by AWS Truewind and site-screening tools that took into account the estimated turbine output, distance to transmission, exclusions, and other factors. The diurnal, seasonal, and dynamic characteristics of the simulated wind speed data have been validated using observations from two met masts in the region, Olga and Wilton; the diurnal and dynamic characteristics of the simulated wind plant output have been validated using data from 8 wind projects. The simulated patterns and dynamic behavior appear to be reasonably consistent with the observations, considering the limitations of the model (particularly grid resolution) and uncertainties in the data. We conclude that the

simulated data should provide a reliable basis for assessing the impacts of integrating large amounts of wind generation on the WAPA grid.